THE JOURNAL OF BIOLOGICAL CHEMISTRY
Vol. 273, No. 50, Issue of December 11, pp. 33472–33481, 1998

Printed in U.S.A.

Protein Inhibitor of Neuronal Nitric-oxide Synthase, PIN, Binds to a 17-Amino Acid Residue Fragment of the Enzyme*

(Received for publication, June 9, 1998, and in revised form, September 28, 1998)

Jing-Song Fan‡, Qiang Zhang‡, Ming Li‡, Hidehito Tochio‡, Toshio Yamazaki§, Masato Shimizu¶, and Mingjie Zhang‡‖

From the ‡Department of Biochemistry, The Hong Kong University of Science and Technology, Clear Water Bay, Kowloon, Hong Kong, People's Republic of China, the §Institute for Protein Research, Osaka University, Suita, Osaka 565, Japan, and the ¶Biomolecular Engineering Research Institute, 6-2-3 Furuedai, Suita, Osaka 565, Japan

Neuronal nitric-oxide synthase (nNOS) is the primary nitric oxide (NO) regulator in neurons. The activity of the enzyme is inhibited by a protein inhibitor called PIN. We were able to purify large quantities of PIN overexpressed in bacterial cells. Analytical ultracentrifugation and chemical cross-linking studies showed that PIN exists as a monomer at low concentrations. The protein forms a high order aggregate at elevated concentrations. We have shown, using NMR spectroscopy, that the previously identified PIN-binding domain (PINB) of nNOS (residues 161–245) adopts a random coil structure in solution. By titrating ^{15}N-labeled PINB with unlabeled PIN, the PIN-binding region of nNOS was precisely mapped to a 17-residue peptide fragment from Met-228 to His-244 of nNOS. NMR titration experiments also showed that PIN binds to nNOS with a 1:2 stoichiometry. A synthetic peptide corresponding to the identified PIN-binding region of nNOS was used to study the interaction between PIN and nNOS in detail. The functional implications of the results obtained from this study are discussed.

Nitric oxide (NO)[1] formed by neuronal nitric-oxide synthase (nNOS) plays major signaling roles in the central and peripheral nervous systems. In the peripheral nervous system, NO functions as a nonadrenergic-noncholinergic neurotransmitter that mediates relaxation of smooth muscles in gastrointestinal and urogenital tracts and in the cerebral circulation (1). NO also acts as a retrograde messenger that regulates synaptic efficacy in the central nervous system. Lowering NO levels by NOS inhibitors blocks hippocampal long-term potentiation, a model of learning and memory (2, 3). Recent experimental evidence has also indicated that NO plays important roles in neuronal development (4–6).

In addition to its physiological roles as a messenger molecule in the peripheral and central nervous systems, NO is also cytotoxic at abnormally high concentrations. In neurons, stimulation of NO synthesis is primarily mediated by the activation of NMDA receptors (2). Overactivity of an NMDA receptor is implicated in a number of neurodegenerative diseases including stroke, Alzheimer's disease, Huntington's disease, and amyotrophic lateral sclerosis (7, 8). Neuronal NOS selective inhibitor was shown to protect brain from ischemic injury (9). Moreover, nNOS knock-out mice exhibit increased resistance to excitotoxicity following focal cerebral ischemia (10). Neuronal cell cultures from nNOS-deficient mice are resistant to NMDA-mediated neurotoxicity (11).

Given both the good and bad properties of NO in neuronal signaling, it is essential that NO synthesis is tightly regulated. NO is synthesized from L-Arg by a complicated chemical reaction catalyzed by three isoforms of NOSs, namely nNOS, endothelial NOS (eNOS), and inducible NOS (iNOS). Neuronal NOS is the primary regulator of neuronal NO concentration and is a Ca^{2+}-calmodulin-dependent enzyme (12). Dual immuno-electron microscopic studies have shown that nNOS co-localizes with NMDA receptors in many neuronal cells (13). The association of nNOS with NMDA receptors is mediated by postsynaptic density-95 (PSD-95) and PSD-93 using PDZ domains of the proteins (14, 15). Co-localization of nNOS and NMDA receptors ensures that Ca^{2+} influx through NMDA receptors is selectively coupled to nNOS activity.

Because abnormally high concentrations of NO are neuronal toxic, it is natural that neuronal cells contain an NO level down-regulation mechanism(s) in addition to the NMDA-coupled up-regulation mechanism. Recently, a protein inhibitor, designated as PIN, was discovered to specifically inhibit nNOS (16). PIN contains 89 amino acid residues and is highly stable in solution.[2] The binding of PIN to nNOS destabilizes the dimeric structure of nNOS and thereby inhibits the enzyme activity (16). The specificity of nNOS inhibition by PIN originates from the fact that the PIN binding domain of nNOS (amino acid residues 161–245) is absent from eNOS and iNOS (16). The expression levels of PIN and nNOS are nearly parallel in different brain regions, supporting the idea that PIN may function as an *in vivo* nNOS activity regulator (17). Following global ischemia, the PIN level rapidly increases in the brain regions that are resistant to ischemic damage (18). The induction of PIN expression following global ischemia presumably counteracts the rise of nNOS activity, thereby protecting neu-

* This work was supported by a grant from the Research Grant Council of Hong Kong (to M. Z.). The NMR spectrometer used in this work was purchased with funds from the Biotechnology Research Institute of HKUST. The costs of publication of this article were defrayed in part by the payment of page charges. This article must therefore be hereby marked "*advertisement*" in accordance with 18 U.S.C. Section 1734 solely to indicate this fact.

‖ To whom correspondence should be addressed. Tel.: 852-2358-8709; Fax: 852-2358-1552; E-mail: mzhang@uxmail.ust.hk.

[1] The abbreviations used are: NO, nitric oxide; NOS, nitric-oxide synthase; nNOS, neuronal NOS; eNOS, endothelial NOS; iNOS, inducible NOS; DLC, dynein light chain; DSG, disuccinimidyl glutarate; DTT, dithiothreitol; GSH, reduced glutathione; GST, glutathione *S*-transferase; IPTG, isopropyl β-D-thiogalactopyranoside; PIN, protein inhibitor of nNOS; PINB, PIN-binding domain of nNOS from residues 161 to 245; PSD, postsynaptic density; PAGE, polyacrylamide gel electrophoresis; CSI, chemical shift index; HSQC, heteronuclear single quantum coherence; NOE, nuclear Overhauser enhancement; NOESY, NOE spectroscopy; TOCSY, total correlation spectroscopy; DFDNB, 1,5-difluoro-2,4-dinitrobenzene; DSG, disuccinimidyl glutarate; PCR, polymerase chain reaction; NTA, nitrilotriacetic acid; NMDA, *N*-methyl-D-aspartate.

[2] M. Zhang, unpublished data.

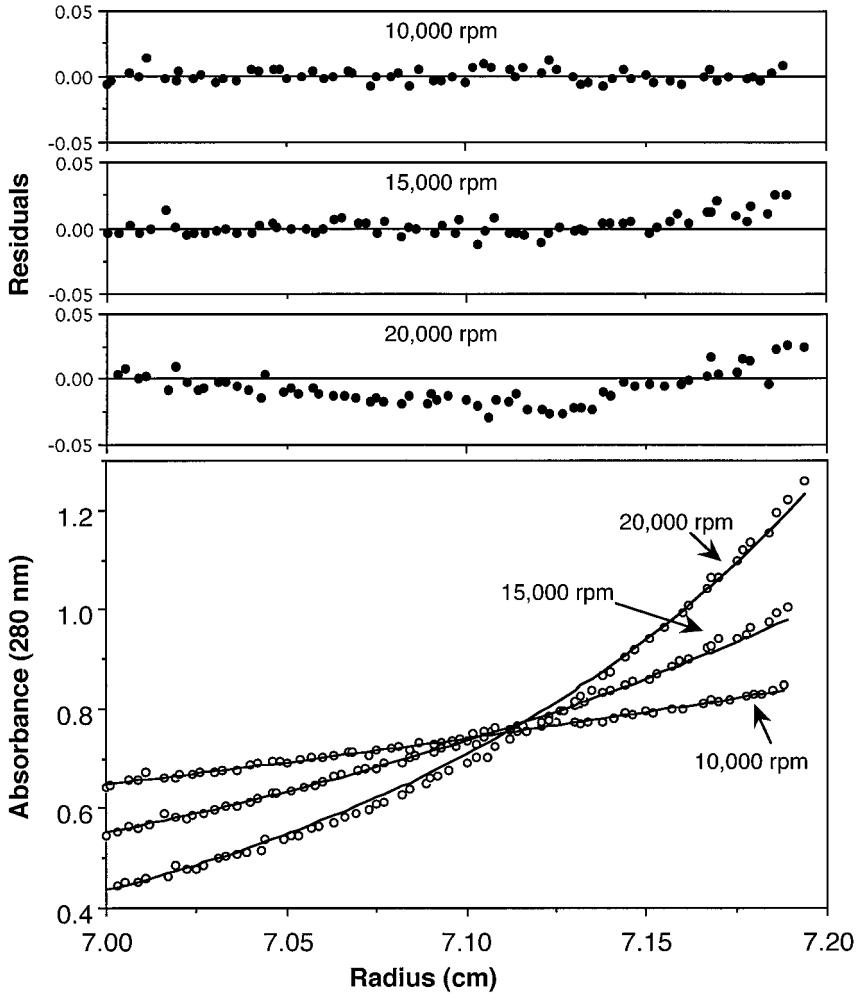

FIG. 1. **Sedimentation equilibrium of PIN shows that it exists as a monomer-trimer equilibrium.** Sedimentation data for 0.05 mM PIN at three different speeds were fitted using a monomer-trimer model. The fitting residuals for each speed are also presented.

rons from excess NO-induced damage.

In this study, we obtained large quantities of pure PIN from a bacterial overexpression system. The protein was shown to exist as a monomer to trimer equilibrium in solution by various biochemical approaches. We have also shown, using NMR spectroscopy, that the previously identified PIN-binding domain of nNOS (amino acid residues 161–245) adopts a random coil structure in solution. The PIN-binding domain of nNOS was mapped to a 17-residue peptide fragment by a combination of NMR spectroscopy and truncation mutations. The results obtained in this work provide insights into the nNOS inhibition mechanism by PIN.

MATERIALS AND METHODS

The 18-residue synthetic peptide (MKDTGIQVDRDLDGKSHK) corresponding to Met-228 to Lys-245 of nNOS was synthesized by the Peptide Synthesis Laboratory, University of Waterloo, Ontario, Canada. The purity of the peptide was greater than 95% as judged by analytical high performance liquid chromatography and mass spectrometry. Because of the lack of aromatic amino acid residues, the concentration of peptide was determined by NMR spectroscopy using the amino acid Tyr as an internal reference.

Cloning, Expression, and Purification of PIN—The rat PIN gene was PCR amplified from rat brain cDNA using the following two primers: 5′-GGAATTCCATATGTGCGACCGGAAGG-3′ (coding strand) and 5′-GCGGATCCTTAACCAGATTTGAACAGGAG-3′ (noncoding strand). The amplified PIN fragment was inserted into the *Nde*I-*Bam*HI sites of the plasmid pET-14b (Novagen). The pET-14b plasmid harboring the PIN gene was then transformed into *Escherichia coli* BL21(DE3) host cells. To express PIN, host cells containing the PIN plasmid construct were grown in LB medium at 37 °C till the A_{600} reached ≈1.0. PIN expression was induced by the addition of IPTG to final concentration of 0.5 mM, and the culture temperature was decreased to 30 °C. Protein expression lasted for 8 h. Uniformly ^{15}N-labeled PIN were prepared by growing the bacteria in M9 minimal medium using $^{15}NH_4Cl$ (1 g/liter) as the sole nitrogen source.

Recombinant PIN was purified by a combination of a Ni^{2+}-NTA affinity column and other chromatographic techniques. Cell pellets were resuspended in 20–30 ml of Ni^{2+}-NTA column binding buffer (20 mM Tris-HCl, pH 7.9, 5 mM imidazole, 0.5 M NaCl) containing 1 mM phenylmethylsulfonyl fluoride, 1 μg/ml leupeptin, and 1 μg/ml antipain. Cells were lysed by a French Press, and the lysate was centrifuged at 30,000 × *g* for 30 min. Soluble PIN in the supernatant was purified on the Ni^{2+}-NTA column following the instructions of the manufacturer (Novagen). The His-tagged PIN eluted from the Ni^{2+}-NTA column was directly applied to a Sephacryl 200 gel filtration column (Amersham Pharmacia Biotech) to remove small amounts of contaminant proteins. His-tagged PIN was eluted with 50 mM Tris-HCl buffer at pH 7.5 containing 1 mM EDTA, 1 mM DTT, and 0.6 M KCl. The fractions containing PIN were combined and dialyzed overnight against 25 mM PO_4^{3-} buffer containing 1 mM DTT at pH 6.5. The N-terminal His-tag was then cleaved by incubating His-PIN with thrombin (1 unit of enzyme per mg of PIN for 8 h). The His-tag and PIN mixture was loaded on to a CM-Sepharose column equilibrated with 25 mM PO_4^{3-} buffer at pH 6.5. PIN was then eluted by a linear NaCl gradient from 0 to 1 M. The purified PIN was extensively dialyzed against 10 mM NH_4CO_3 buffer, freeze dried, and stored at −80 °C.

Cloning, Expression and Purification of PINB—The rat PIN-binding domain (PINB) of nNOS encompassing amino acid residues 161 to 245 was cloned from rat brain cDNA by PCR using a pair of primers: 5′-GCGGATCCCATGCCCAAGGCCATG-3′ (coding strand) and 5′-GCGGATCCTATTTGTGCGATTTGCCATC-3′ (noncoding strand). The PCR-amplified fragment was inserted into the *Bam*HI-*Eco*RI sites of the GST-fusion vector pGEX-2T (Amersham Pharmacia Biotech). The PINB containing pGEX-2T plasmid was then transformed into BL21(DE3) *E. coli* host cells (Novagen) for large scale protein expression. Various PINB truncation mutants fused with GST were generated in a similar manner using PCR. To express PINB and its truncated

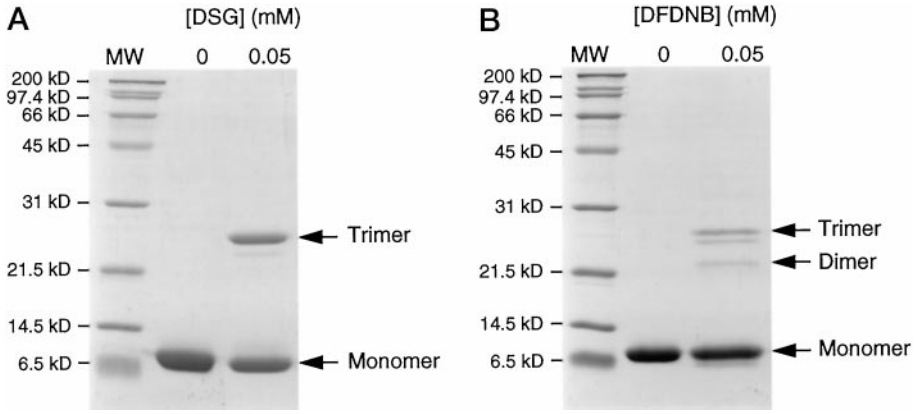

FIG. 2. **Chemical cross-linking of PIN by DSG and DFDNB.** Purified PIN (0.5 mg/ml) was treated with 0 or 0.05 mM of DSG (*A*) or DFDNB (*B*). The reactions were quenched by the addition of 0.5 M Tris, pH 7.0. The samples were subjected to 15% SDS-PAGE analysis, and the gel was stained with Coomassie Blue.

forms, host cells containing the PINB plasmids were grown in LB medium at 37 °C to $A_{600} \approx 1.0$ before the addition of IPTG (0.5 mM final concentration). The expression of the proteins lasted for 3 h at 37 °C, and the cells were then harvested by centrifugation. Uniformly ^{15}N- and ^{15}N/^{13}C-labeled PINB were prepared by culturing the bacteria in M9 minimal medium using $^{15}NH_4Cl$ (1 g/liter) as the sole nitrogen source or $^{15}NH_4Cl$ (1 g/liter) and $^{13}C_6$-glucose (1 g/liter) as the sole nitrogen and carbon sources, respectively.

GST-fused full-length PINB and its truncated mutants were purified using GSH-Sepharose affinity columns (Amersham Pharmacia Biotech) following the instructions of the manufacturer. The purified GST-fusion proteins were dialyzed against 100 mM sodium phosphate buffer containing 1 mM DTT, pH 7.5, to remove GSH, and the protein samples were directly used for PIN-binding assay. Full-length PINB was released from GST-PINB by thrombin digestion while the fusion protein was bound to the affinity column (digested with 3 units of thrombin per mg of GST-PINB for 3 h at room temperature). The supernatant containing PINB was passed through a Sephacryl-100 gel filtration column to remove thrombin and other small amounts of contaminant proteins (Amersham Pharmacia Biotech), and the fractions containing PINB were found to be pure as judged by a single band on an SDS-PAGE gel (data not shown).

Chemical Cross-linking—To cross-link free amino groups of PIN, the protein sample (final concentration of 0.5 mg/ml) was dissolved in 20 mM HEPES buffer, pH 8.0, in the presence of 50 mM NaCl, 1 mM DTT. The sample was then treated with 0.05 mM DFDNB (Pierce) for 1 h at 30 °C. DFDNB was dissolved in methanol, and the final methanol concentration in cross-linking reactions was 5% (v/v). Cross-linking of PIN with DSG (Pierce) was performed identically, except that DSG was dissolved in *N*,*N*-dimethylformamide, and the reaction was carried out at 20 °C for 30 min.

Analytical Ultracentrifugation—Sedimentation equilibrium experiments were conducted using a Beckman Optima XLI analytical ultracentrifuge equipped with an optical detection system. Experiments were carried out using 12-mm path length cells with quartz windows. The centrifugation was run at 10,000, 15,000 and 20,000 rpm at 20 °C for 12 h at each speed. Samples were considered at equilibrium when sequential scans 2 h apart were superimposable. The protein was dissolved in 100 mM potassium phosphate buffer containing 1 mM DTT, pH 6.0, and 100 μl of protein sample was filled in the cell. Data were collected using continuous radial scanning at 280 nm. Partial specific volume was calculated based on the amino acid composition of the protein (19). The data of three different speeds were globally fit with a monomer-*n*mer equilibrium ($nPIN \rightleftharpoons PIN_n$) with the molecular weight of the monomer as a fixed constant. The experimental data were fit using "Multiorg" software provided by Beckman.

PIN Binding Assays of PINB and Its Truncation Mutants—The binding between PIN and various truncated forms of GST-PINB was assayed in 100 mM sodium phosphate buffer containing 1 mM DTT, pH 7.5. Equal molar amounts of PIN and various GST-PINB samples (0.6 nmol each) were mixed in 30 μl of the assay buffer. The GST-PINB/PIN complexes were precipitated by 10 μl of fresh GSH-Sepharose beads. The pellets were washed three times with 300 μl of the assay buffer, and the washed pellets were boiled with 30 μl of 2× SDS-PAGE sample buffer. The intensity of the PIN band on SDS-PAGE gels was used to judge the binding between PIN and various truncated forms of PINB.

NMR Experiments—All NMR spectra were recorded on a Varian UNITY Inova 500 MHz NMR spectrometer equipped with a pulse field gradient driver and a *z*-axis actively shielded ^{1}H(^{13}C,^{15}N)-triple resonance probe head. The temperature of all NMR experiments was maintained at 30 °C.

A ^{15}N-labeled and a ^{15}N/^{13}C-labeled PINB sample, dissolved in 90% H_2O, 10% D_2O containing 100 mM potassium phosphate, pH 6.0, were prepared for the sequential backbone assignment of the protein. Sensitivity-enhanced ^{1}H-^{15}N-HSQC (20), HNCACB (21), and CBCA-(CO)NH (22) experiments were recorded for the sequence-specific backbone resonance assignment of PINB. The sequential assignment was further confirmed by a pair of ^{15}N-separated three-dimensional-TOCSY (mixing time = 71.5 msec), and three-dimensional-NOESY (mixing time = 100 msec) experiments recorded on a ^{15}N-labeled PINB sample (23). All NMR data were processed and displayed using the NMRPipe software package (24).

To study the conformational changes of PINB induced by PIN-binding, a ^{15}N-labeled PINB sample (≈1.0 mM) was titrated with an unlabeled PIN stock solution (≈2.0 mM concentration) at a 0.1 molar ratio interval. A ^{1}H-^{15}N-HSQC spectrum was recorded at each titration point to monitor spectral changes exclusively originated from PINB during the titration. The conformational changes of PIN resulting from PINB (or the 18-residue synthetic peptide) binding were studied by titrating ^{15}N-labeled PIN (≈1.5 mM concentration) with an unlabeled PINB (the nNOS peptide) stock solution (≈4 mM) in a similar manner.

RESULTS

Expression and Purification of PIN—Various expression conditions were tested to optimize the expression of PIN. It was found that induction of PIN expression at 30 °C for a duration of approximately 8 h gave rise to the highest yield of PIN in the soluble form. Purification of PIN was relatively straightforward. Pure His-tagged PIN was obtained by using a gel filtration column following Ni^{2+}-NTA affinity chromatography. The His-tag cleaved by thrombin was removed from PIN by a cation-exchange column (data not shown). An ~25-mg quantity of pure PIN was purified from 1 liter of LB medium. About half that quantity of PIN was obtained when the expressing strain was grown in M9 minimal medium for stable isotope labeling. The PIN samples used throughout this study contained three extra residues ($G^{-3}S^{-2}H^{-1}$) resulting from a cloning artifact. High yield expression and successful purification of PIN has enabled detailed structural and functional studies by various biochemical and biophysical techniques.

Monomer-Trimer Equilibrium of PIN in Solution—The elution profile of the gel filtration chromatography during PIN purification indicated that PIN has a molecular mass over 25 kDa, indicating that the protein is not a pure monomer in solution (data not shown). Initial NMR experiments also indicated that the line width of the protein is significantly broader than a monomeric protein with 89 amino acid residues, suggesting that the protein may form higher order aggregates at elevated concentrations (data not shown).

Sedimentation equilibrium experiments were carried out to determine the self-association of PIN in different concentrations. At low protein concentrations (<0.01 mM), the data can be fitted well by treating PIN as a monomer (data not shown).

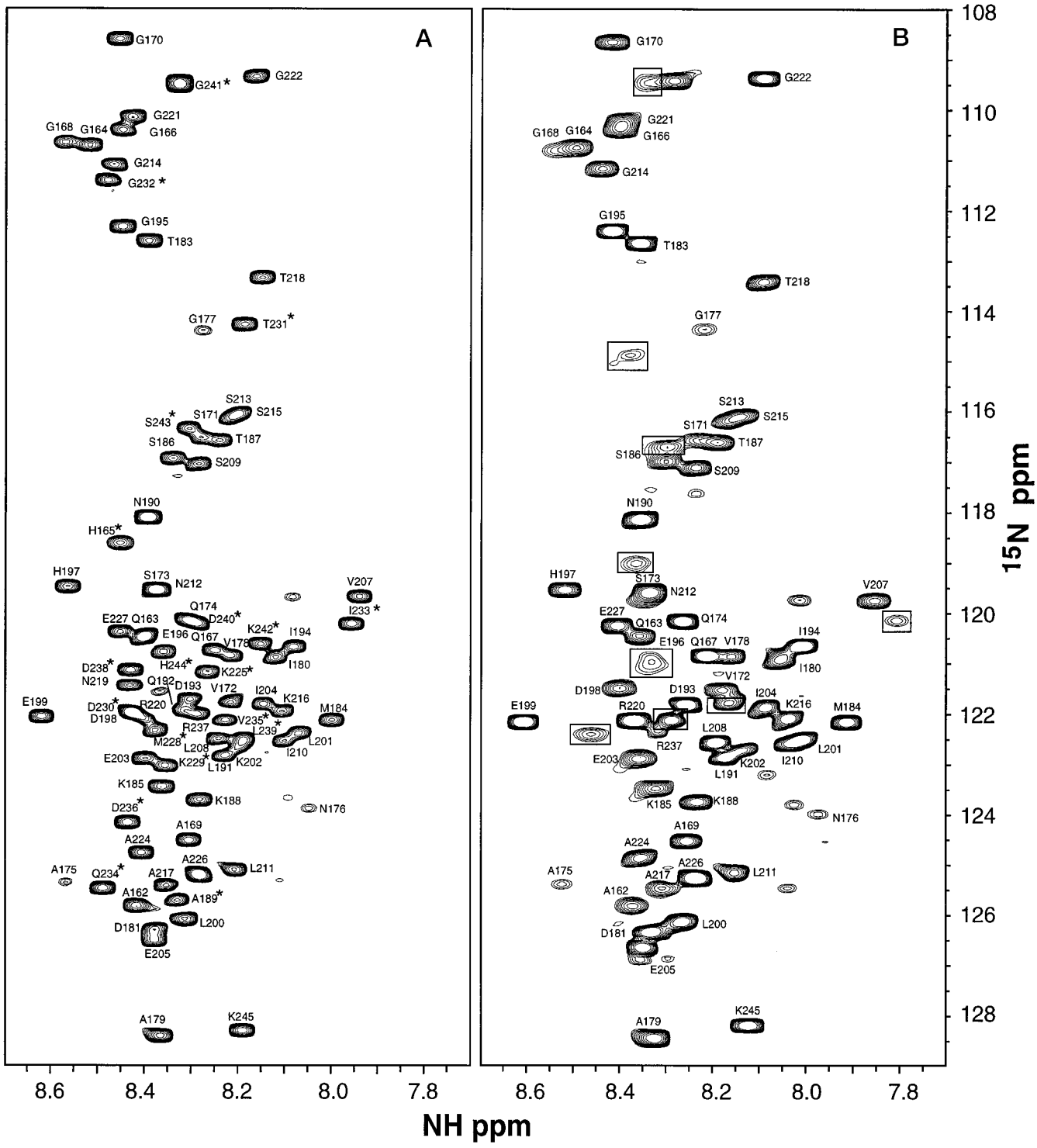

FIG. 3. **^{1}H-^{15}N-HSQC spectrum of free PINB (*A*) and PIN-bound PINB (*B*).** The assignments in both panels are labeled with respective amino acid residue names and numbers. The amino acid residues of ^{15}N-labeled PINB that undergo chemical-shift and peak intensity changes during the PIN titration are labeled with *asterisks* in *panel A*. The newly formed peaks originated from PINB at the end of the titration are *highlighted* with *open boxes* (*panel B*).

However, when the protein concentration increases, fitting the data to a monomer or a dimer gives poor fits with large non-random residuals. Rather, the data for PIN at 0.03 mM or higher fit best to a monomer-trimer equilibrium. Fig. 1 shows the representative fitting result of a sedimentation experiment at an initial PIN concentration of 0.05 mM using a monomer-trimer equilibrium model. The result strongly indicates that PIN exists as a monomer-trimer equilibrium at high concentrations.

The monomer-trimer equilibrium of PIN suggested by hydrodynamic studies was further confirmed by chemical cross-linking studies. An amine-selective chemical cross-linking reagent, DSG (with a linking spacer length of 7.7 Å), was used to probe the formation of higher order structure of PIN. As shown in Fig. 2*A*, a sharp band with a molecular weight of ≈27 kDa can be observed in the DSG-treated protein sample. This 27-kDa band protein presumably represents the cross-linked trimer of PIN as the monomeric PIN migrates at ≈9 kDa. We have also used

another amine-selective cross-linker, DFDNB, to covalently link PIN. In contrast to DSG, DFDNB has a much shorter spacer arm (3 Å). Therefore, cross-linking by DFDNB requires two lysine residues of PIN to be in close proximity with each other. As expected, the DFDNB-mediated cross-linking reaction occurs more slowly than that mediated by DSG. In DFDNB-treated PIN, a 27-kDa protein band corresponding to the cross-linked trimer can be detected (Fig. 2*B*). In addition to this 27-kDa band, a 22-kDa band is also visible, and this 22-kDa band may represent the cross-linked dimer of the protein. The formation of cross-linked dimer by DFDNB may indicate that a pair of lysine residues from two subunits of the trimeric PIN are particularly close in space.

PINB Adopts a Random Coil Structure in Solution—To better understand the interaction between PIN and PINB, we set out to determine the three- dimensional structure of PINB by NMR spectroscopy. Fig. 3*A* shows the ^{1}H-^{15}N-HSQC spectrum of ^{15}N-labeled full-length PINB in 100 mM potassium phosphate buffer, pH 6.0. All of the amide protons have a chemical shift dispersion within 0.7 ppm (from 7.9 to 8.7 ppm), and ^{15}N resonances have a chemical shift distribution less than 20 ppm (108.5 to 128.5 ppm). Such narrow chemical shift dispersions (particularly the amide protons) strongly indicate that PINB is likely to adopt a random coil structure in solution.

To prove that PINB indeed adopts a random coil structure in solution, we carried out backbone sequence-specific assignment of PINB by heteronuclear multi-dimensional NMR experiments. The combination of a pair of CBCA(CO)NH and HNCACB triple resonances experiments using a $^{15}N/^{13}C$-labeled PINB allowed us to obtain near complete sequence-specific backbone assignment of the protein (assignment available from the authors). The sequential assignment obtained from the triple resonance experiments was further confirmed by a pair of three-dimensional ^{15}N-separated TOCSY and NOESY experiments recorded with a ^{15}N-labeled PINB (data not shown).

After completing the sequence-specific assignment, we analyzed the NOE connections of PINB using data obtained from the ^{15}N-separated three-dimensional NOESY experiment. No medium and long range backbone NOE connectivities were observed throughout the protein, indicating that PINB has a random coil structure in solution (data not shown). Other than the NOE connectivities, chemical shift values are particularly informative for determining secondary structures of proteins (25). Fig. 4 shows the $^{1}H_{\alpha}$ and $^{13}C_{\alpha}$ chemical shift index (CSI) values plotted as a function of amino acid residues of PINB. It is clear that no regular secondary structural elements can be observed in PINB. Taken together, both NOE connectivities and CSI data show that the 85-residue PINB adopts a random coil structure in solution.

PIN Binds to a 17-Amino Acid Residue Fragment of nNOS—To study the interaction between PIN and PINB and conformational changes of PINB induced by PIN binding, we titrated ^{15}N-labeled PINB with unlabeled PIN. A ^{1}H-^{15}N-HSQC spectrum was recorded at each titration point to selectively observe the spectral changes of PINB resulting from the PIN binding. During the titration, the intensities of a selected set of peaks gradually decrease (peaks labeled with *asterisks* in Fig. 3*A*), and a new set of resonances appear at completely different chemical shift values (the peaks highlighted with *open boxes* in Fig. 3*B*). The newly appeared peaks presumably represent amino acid residues of PINB that are directly involved in the interaction with PIN. The titration had completed when a half-equivalent amount of PIN was added to the PINB solution, indicating that PIN binds to PINB at a 1:2 stoichiometry. The co-existence of the resonances originating from the free and PIN-bound forms of PINB during the titration demonstrates that two forms of PINB are in a slow chemical change process. Such slow chemical exchange between free PINB and PIN-bound PINB indicates that PIN binds to PINB with a high affinity ($K_d < 10^{-6}$ M by assuming a near diffusion controlled on-rate of PINB and the nNOS peptide below). The fact that the GST-PINB/PIN complex could stand the extensive wash of the binding assay buffer also supports that PIN binds to PINB with a K_d value of 10^{-6} M or lower (Fig. 5). The newly appeared peaks seen in Fig. 3*B* have significantly broader line widths compared with the peaks in Fig. 3*A*, consistent with the fact that the PIN/$PINB_2$ complex has a much larger molecular mass than PINB alone (28 *versus* 8.5 kDa). Other than the small set of peaks that disappear during the PIN titration, the rest of the resonances exhibit neither chemical shift nor intensity changes (Fig. 3), indicating that only a small part of PINB is involved in PIN binding. By taking advantage of the sequence-specific assignment obtained above, we were able to locate the amino acid residues that show peak intensity and chemical shift changes during the titration. The residues that are labeled with *asterisks* in Fig. 3*A* correspond to a continuous stretch of 17 amino acid residues (Met-228 to His-244) at the very C-terminal tail of PINB, and this 17-residue peptide fragment is likely to represent the PIN-binding domain of nNOS.

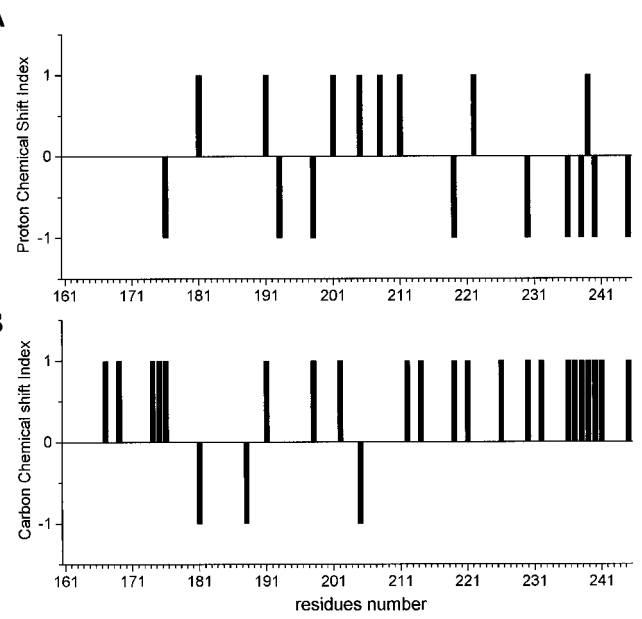

FIG. 4. **Plot of $^{1}H_{\alpha}$ (*A*) and $^{13}C_{\alpha}$ (*B*) CSI values as a function of amino acid residue number of PINB.** When the $^{1}H_{\alpha}$ chemical shift of an amino acid residue up-field (or down-field) shifts more than 0.1 ppm, its CSI value is assigned to −1 (or +1). Similarly, when $^{13}C_{\alpha}$ chemical shift of a residue shifts to down-field (or up-field) more than 0.7 ppm, its CSI value is assigned to +1 (or −1) (25). Together with the NOE pattern derived from the three-dimensional ^{15}N-separated NOESY experiment, we conclude that PINB adopts a random coil structure in solution.

To confirm the result of the PIN-binding region identified from the NMR experiments, we created a series of N- and C-terminal truncation mutants of PINB in their respective GST-fusion forms (Fig. 5). These GST-fusion proteins were then assayed for their PIN-binding ability, and the result is shown in Fig. 5. It is clear from the data that the C-terminal ten residues of PINB are absolutely required for PIN-binding, as deletions of ten or more amino acid residues from the C-terminal end of PINB completely abolished its PIN-binding capability, whereas deletions up to 40 amino acid residues from the N terminus had no effect on the PIN-binding. Therefore, the PIN-binding domain of PINB is located within the C-ter-

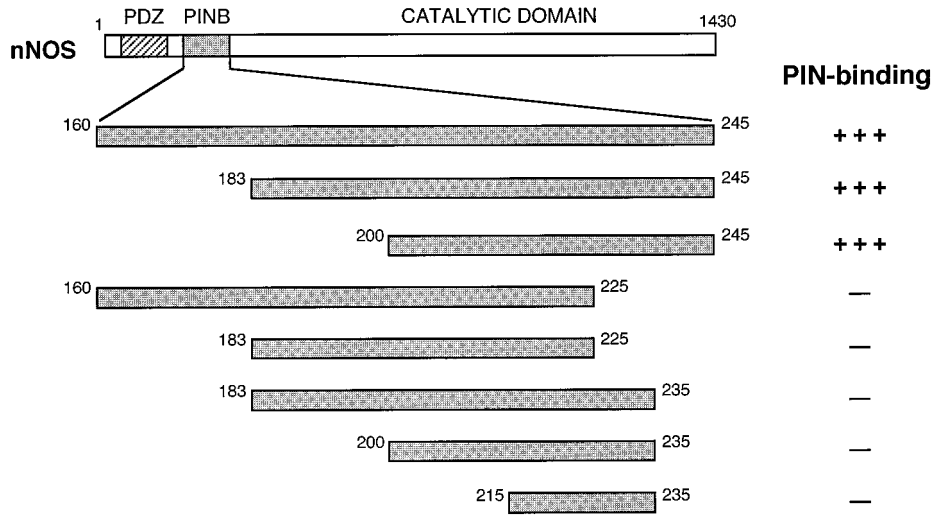

FIG. 5. **PIN binding assay results of the various truncation mutants of PINB.** All of the PINB truncation mutations were generated as their respective N-terminal GST-fusion proteins, and the GST-PINB/PIN complexes were precipitated by GSH-Sepharose beads. The intensities of the PIN band on SDS-PAGE gel were used to semi-quantitatively estimate the binding ability of various GST-PINB mutants. See "Materials and Methods" for the detailed assay procedure.

minal 45 amino acid residues of the protein. The result obtained from these truncation mutation studies agrees with the conclusion drawn from our earlier NMR experiments.

Binding of PINB Induces Global Conformational Changes of PIN—A similar strategy was used to selectively observe conformational changes of PIN resulting from PINB binding by using unlabeled full-length PINB to titrate with ^{15}N-labeled PIN. Fig. 6 shows representative panels of the ^{1}H-^{15}N-HSQC spectra of ^{15}N-labeled PIN during the titration. Similar to what was observed in the experiment described in Fig. 2, the intensities of free PIN peaks gradually decrease with the addition of increasing amounts of PINB. A new set of resonances, which correspond to the residues of PIN in the complex with PINB, were observed during the titration. This slow chemical exchange process between free PIN and PIN in the complex with PINB agrees with our earlier conclusion stating that PIN binds to PINB with a high affinity. Unlike only a small subset of the PINB peaks undergoing intensity and chemical shift changes, essentially every resonance of PIN shows peak intensity decrease during titration and eventually disappears at the end of the titration (Fig. 6). The result indicates that PIN undergoes a global conformational change upon forming the complex with PINB. At the mid-point of titration (see *panel C* in Fig. 6, for example), we observed four peaks for each amino acid residue. The data indicate that PIN may contain two separate binding sites for PINB (see below for details). Extensive line-broadening during the titration using full-length PINB prevented us from a detailed analysis of the interaction between the two proteins. However, we were able to obtain a much clearer picture of the interaction by using a synthetic peptide comprising the PIN-binding region of nNOS (see Fig. 8*A*, for example). When PINB to PIN molar ratio reached 2.0, the resonances of free PIN completely disappeared, and the intensities of the newly formed peaks do not change further (Fig. 6*D*), further substantiating that PIN binds to PINB at a 1:2 stoichiometry. The extremely broad line widths of PIN peaks in the PIN/$PINB_2$ complex consist with a much higher molecular weight of the complex with respect to the free PIN.

The 17-Residue Peptide Fragment from Met-228 to His-244 of nNOS Is Sufficient for Its Binding to PIN—A synthetic peptide was used to further prove that the 17-residue peptide fragment identified from the NMR titration experiment is sufficient for nNOS to bind to PIN. A lysine residue (corresponding to Lys-245 of nNOS) was added at the C-terminal end of the 17-residue peptide fragment to avoid racimization of the histidine (His-244 of nNOS) during the peptide synthesis. Therefore, an 18-residue synthetic peptide corresponding to Met-228 to Lys-245 of nNOS was used in the subsequent studies, and the peptide was termed as the nNOS peptide. Fig. 7 shows the ^{1}H-^{15}N-HSQC spectrum of ^{15}N-labeled PIN complexed with two equivalents of the nNOS peptide. One can see that the chemical shift distributions of the spectra shown in Fig. 6*D* and Fig. 7 are essentially identical, indicating that PIN adopts the same conformation in the complexes with the full-length PINB and the nNOS peptide. The result also demonstrates that the nNOS peptide represents the complete PIN-binding domain of the enzyme.

The ^{1}H-^{15}N-HSQC spectrum shown in Fig. 7 has a much narrower line width and higher sensitivity compared with the one shown in Fig. 6*D*. We, therefore, repeated the titration experiment shown in Fig. 6 using the synthetic peptide instead of the full-length PINB. Indeed, we were able to observe the spectral changes of PIN during the titration much more clearly. The results further show that the backbone amides of PIN undergo essentially identical chemical shift changes observed when titrating with the full-length PINB. However, the higher sensitivity and narrower line widths of the ^{1}H-^{15}N-HSQC spectra enabled us to monitor changes of individual backbone amides of PIN during the nNOS peptide titration. For clarity, we have chosen two amino acid residues (Asp-37 in the second α-helix and Gly-59 in the second β-strand of the protein, see Ref. 36) to show the spectral changes of PIN during the titration (Fig. 8). A similar pattern was observed for the amino acid residues throughout the protein (data not shown). Upon the addition of a small amount of the nNOS peptide (0.4 equivalent for example, Fig. 8*A*), one notices the intensity decrease of free PIN. At the same time, two new peaks with similar intensities appear with completely different chemical shift values. The intensities of these two newly formed peaks increase with further addition of the nNOS peptide until the amount of the nNOS peptide reached one equivalent of PIN. Further addition of the nNOS peptide leads to a gradual decrease of the peak intensities and eventual disappearance of these two peaks. In the middle of the titration (*e.g.* at 0.8 equivalent of the nNOS peptide shown in Fig. 8*A*), a third peak appears for each amino acid residue, and the intensity of this peak steadily increases until the end of the titration, where two equivalents of the nNOS peptide were added to the PIN sample (Fig. 8*A*). At the end of titration, only one peak for each amino acid residue is observed (Fig. 7 and 8), indicating that the final complex has one single conformation. Because PIN binds two equivalents of the nNOS peptide, we propose that the two newly appeared peaks for each amino acid residue at the beginning of the titration represent two PIN, and the nNOS peptide complex intermediates with each has one peptide bound (Fig. 8*B*). The

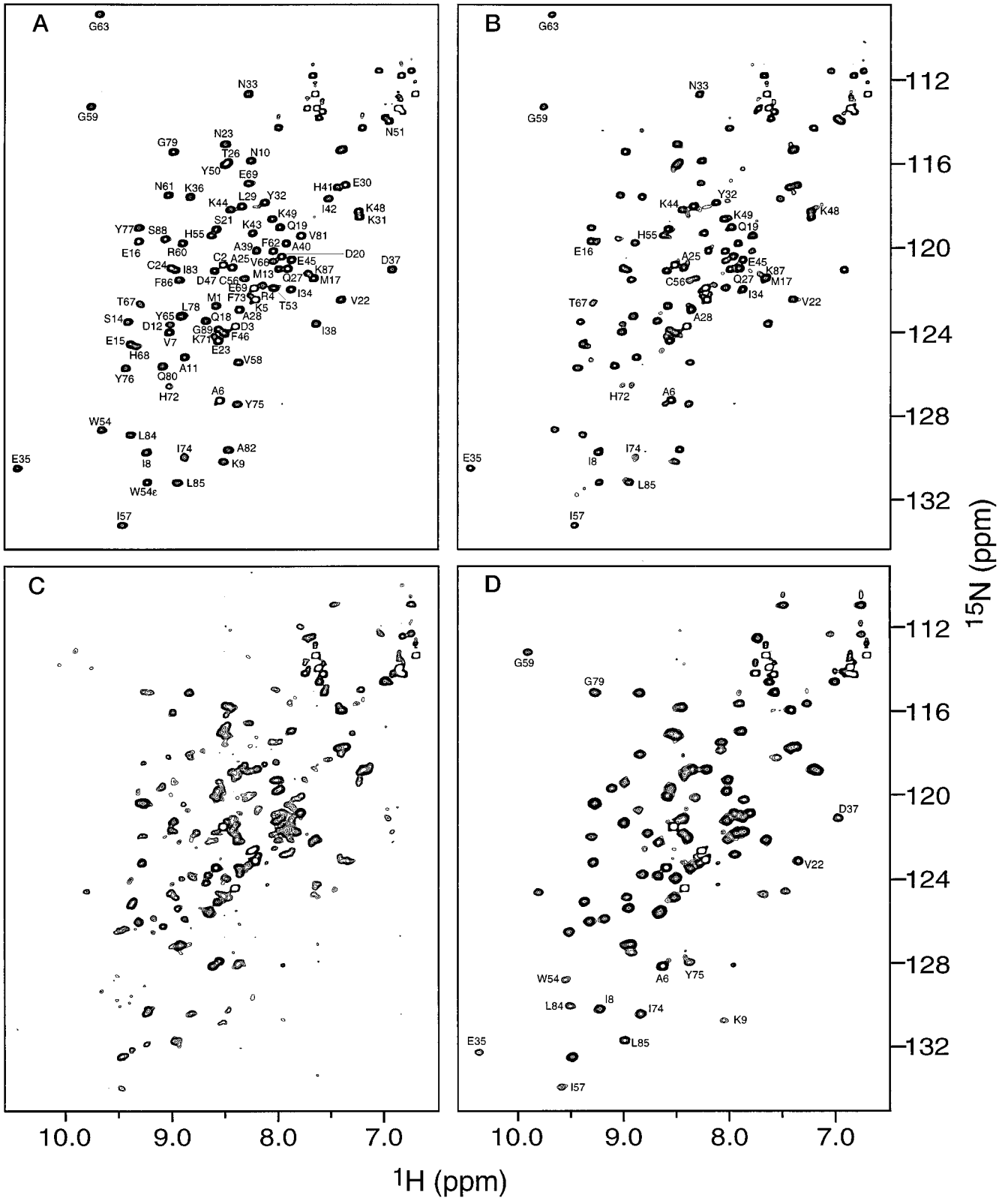

FIG. 6. **^{1}H-^{15}N-HSQC spectra of ^{15}N-labeled PIN at different PINB titration points.** *A*, free PIN; *B*, with 0.4 eq of unlabeled PINB; *C*, with 1.0 eq of PINB; and *D*, with 2.0 eq of PINB. The assignments of PIN in *panel A* are labeled with amino acid names and residues (H. Tochio and M. Zhang, unpublished data). The spectra shown in *panels A*, *B*, and *C* were collected with 8 scans, and the spectrum in *panel D* was recorded with 64 scans.

near equal peak intensities observed for the intermediates indicate that the two nNOS binding sites of PIN have similar affinities and are seemingly independent of each other. The third peak observed for each backbone amide at higher molar ratios of the nNOS peptide to PIN represents the final complex of PIN, with two molecules of the peptide bound. A schematic diagram is drawn to illustrate the titration process of PIN by the nNOS peptide (Fig. 8*B*).

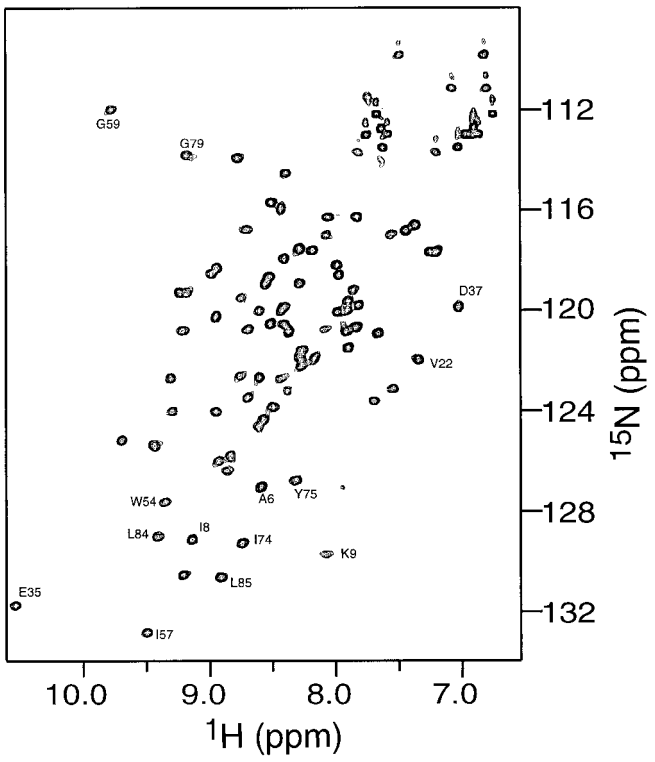

FIG. 7. **^{1}H-^{15}N-HSQC spectra of ^{15}N-labeled PIN complexed with 2.0 eq of the nNOS peptide.** Partial assignment were obtained and labeled in the figure.

DISCUSSION

In this study, we have successfully expressed and purified large quantities of PIN for NMR and biochemical studies. Various biochemical and biophysical approaches have shown that PIN exists as a monomer at low concentrations. At elevated protein concentrations, the protein forms higher order aggregates via self-association. NMR relaxation studies showed that PIN (1.5 mM concentration) has a correlation time (τ_m) of 13.5 ns at 30 °C and that this correlation time also corresponds to a trimer state of the protein.[3] The trimer structure observed in this study is in contradiction with an earlier report that a PIN homologue (or the dynein light chain, DLC) exists as a dimer (26). The detection of a molecular mass ≈20-kDa band in DFDNB-treated DLC led the authors to conclude that the protein forms a dimer (26). In our study, very low concentration of cross-linker (0.05 mM DSG) and low protein concentration (0.5 mg/ml) were used to eliminate possible nonspecific cross-linking reactions that might happen. A sharp, reproducible reaction product with a molecular mass of ≈27 kDa can be observed in DSG cross-linked PIN (Fig. 2*A*). The result clearly shows that PIN is not a dimer in solution. As shown in Fig. 2*B*, cross-linking of PIN by a very short space arm cross-linker such as DFDNB can produce misleading results, as both dimer and trimer are observed in the reaction products. We have also tried to cross-link PIN by disulfide bond formation. Analogous to DFDNB, formation of inter-subunit disulfide bond requires two free Cys residues in close proximity. Dimer form of PIN was the dominant product in the disulfide cross-linked protein (data not shown). Therefore, caution should be taken in interpreting cross-linking results when one uses those cross-linking reagents with short space arms. However, some of the chemical cross-linking experiments of DLC were carried out *in situ* (26), and it is possible that the protein exists as a dimer under special cellular conditions.

In contrast to eNOS and iNOS, nNOS contains an additional 250 amino acid residues at the N-terminal end of the enzyme. Within this N-terminal extension, the first 150-amino acid residues encodes an extended PDZ domain which targets the enzyme to the cell membrane through the postsynaptic density proteins PSD-95 and PSD-93 (14, 15). The peptide fragment consisting of amino acid residues from 161 to 245 was identified to be the PIN-binding domain of the enzyme (16). PIN inhibits nNOS by destabilizing the dimeric structure of the enzyme. The specificity of PIN in inhibiting nNOS originates from the fact that amino acid residues form 161 to 245 of nNOS are absent in eNOS and iNOS. In this work, we showed that the 85-residue nNOS fragment (amino acid residues 161 to 245), corresponding to the previously identified PIN-binding domain of the enzyme, adopts a random coiled structure in solution. A closer inspection of the amino acid sequence shows that PINB does not contain any aromatic amino acid residues. In addition, the occurrence of other hydrophobic amino acid residues (Ile, Leu, Met, Val, and Ala) is also below the average amount found in proteins (27). The complete lack of aromatic amino acid residues and low occurrence of other hydrophobic amino acids may prevent PINB from folding into a compact three-dimensional structure that normally contains a hydrophobic core. It is likely that the PINB fragment in nNOS also adopts a random coil structure as it can function as a relatively independent unit to bind to PIN (16). If this is the case, the N-terminal PDZ domain is connected with the catalytic domain of enzyme with a long flexible linker (Fig. 9). Such a long flexible link should ensure that the bulky catalytic domain will not restrict the localization of the enzyme to the cell membrane via its PDZ domain.

Because PINB is completely unstructured in solution, it is unlikely that every amino acid residue is required for its binding to PIN. By using unlabeled PIN to titrate ^{15}N-labeled PINB, we have been able to determine that a 17-residue peptide fragment located at the C-terminal end of PINB (from residue Met-228 to His-244) encompasses the complete PIN-binding region of nNOS. The rest of PINB remains as a random coil structure upon formation of the complex with PIN as neither the chemical shifts nor peak intensities of these residues change during the titration (Fig. 3). The result obtained from NMR experiments agrees well with that from truncation studies. However, the NMR titration experiment was not merely a redundant confirmation of the result obtained from the mutational studies. Rather, the NMR studies allowed us to accurately and quickly locate the PIN-binding region of nNOS to individual amino acid residues. Indeed, we have been able to prove, using a synthetic peptide, that the 17-residue peptide fragment contains the complete PIN-binding domain of nNOS. In principle, such chemical-shift perturbation studies can be a general strategy in mapping the binding regions in protein-protein interactions.

The slow chemical exchange processes observed in both NMR titration experiments and *in vitro* binding assay experiments have shown that PIN binds to PINB with a high affinity (Figs. 3, 5, 6, and 8). The broad line width seen in the complex of PIN with the full-length PINB (Fig. 6*D*) is likely resulted from a large molecular weight of the complex (≈28 kDa). The good chemical shift dispersion, high sensitivity, and narrow line width shown in Fig. 7 suggest that PIN forms a stable complex with the nNOS peptide. One should be able to assign all the resonances and then determine the three-dimensional structure of the PIN/the nNOS peptide complex by NMR spectroscopy. The superb sensitivity and resolution of the titration experiments using the nNOS peptide allowed us to identify the existence of two independent nNOS binding sites on PIN (Fig.

[3] K. H. Sze and M. Zhang, unpublished data.

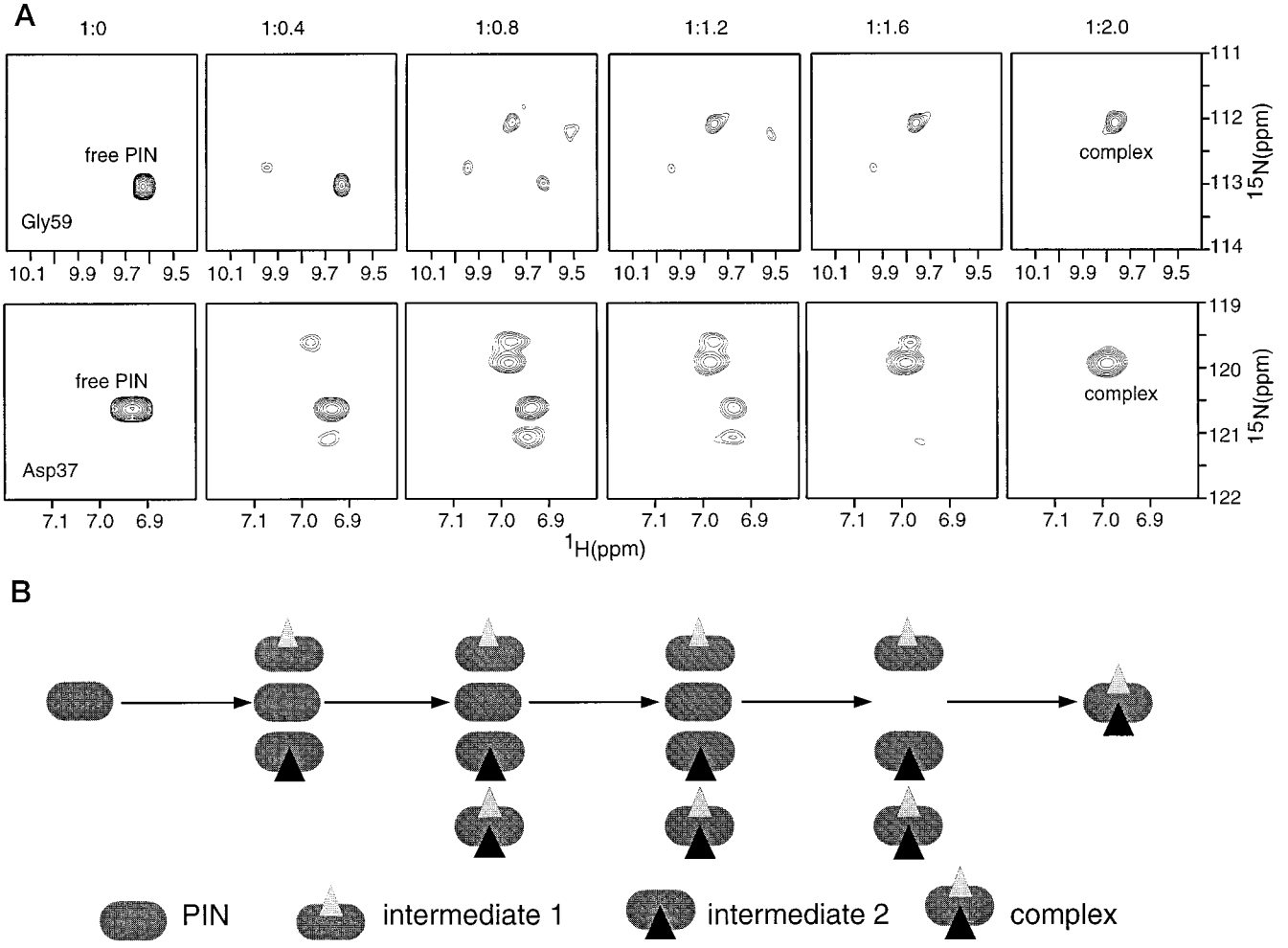

FIG. 8. *A*, representative regions of ^{1}H-^{15}N-HSQC spectra of ^{15}N-labeled PIN at different titration points of the nNOS peptide. The molar ratios of PIN to the nNOS peptide at each titration point are indicated on the *top* of the *spectra*. *B*, a schematic model illustrating the interaction between PIN and the nNOS peptide during the titration.

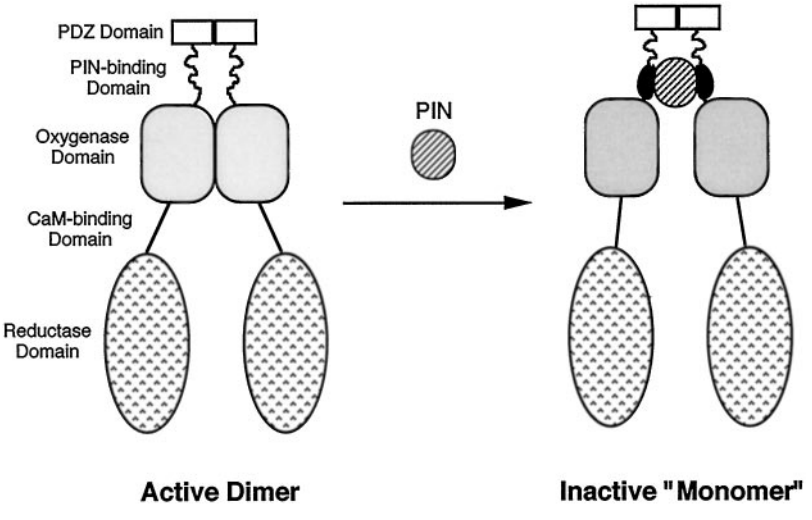

FIG. 9. **A schematic model showing the inhibition mechanism of nNOS by PIN.** In this model, the reductase domain and the oxygenase domain of nNOS are connected by the calmodulin-binding domain. The 86-residue flexible PINB links the PDZ domain and the oxygenase domain of the enzyme. The active enzyme is a dimer which is formed primarily through its oxygenase domain. In addition, the PDZ domain of nNOS also forms a homodimer (Q. Zhang and M. Zhang, unpublished data). The binding of PIN induces conformational changes to the region immediately N-terminal to the oxygenase domain of the enzyme and thereby destabilizes its dimeric structure.

8). Preliminary experimental data have suggested that the solvent-exposed hydrophobic surface of PIN is involved in nNOS binding (36).[4] A detailed picture awaits the three-dimensional structure of the complex to be solved, and such work is in progress in our laboratory.

In addition to its interaction with nNOS, PIN and its homologues in other species were also found to bind to other proteins including cytoplasmic dynein complex (28, 29) and myosin V (30). The extraordinary high sequence conservation of PIN

[4] J-S. Fan and M. Zhang, unpublished data.

among different species suggests that the protein may act as a multifunctional regulatory protein (36). The three-dimensional structure of PIN was recently determined (36). The protein contains a large solvent-exposed hydrophobic surface that could serve as the binding region for its targets. The hydrophobic surface of PIN is reminiscent of the hydrophobic surfaces seen in a ubiquitous Ca^{2+} regulatory protein, calmodulin (31). Because the PIN-binding region of nNOS was mapped to a 17-amino acid residue peptide fragment, we searched the protein data base to see whether homologous amino acid sequences can be found in other proteins. To our surprise, no single homologous sequences, other than those in various forms of nNOSs, could be found in the data base. Given that PIN can also bind to a number of other proteins, it is likely that the PIN-binding domains of its various targets have very different amino acid sequences. We further note the similarity between calmodulin and PIN in terms of their respective target interactions. Calmodulin recognizes multiple targets, and the calmodulin-binding domains of these targets comprise a continuous stretch of peptide fragment with ≈20 amino acid residues. In addition, the calmodulin-binding domains of its target proteins do not share obvious sequence homology (31). Hence, we hypothesize that PIN may function as a versatile regulatory protein analogous to calmodulin.

Combining what is known about the interaction between PIN and nNOS, we propose a model in explaining the inhibition of the enzyme by PIN (Fig. 9). The active form of nNOS is a homodimer, and the dimerization is primarily mediated via the oxygenase domain of the enzyme (for a review, see Ref. 32). The x-ray crystal structure of the iNOS oxygenase domain shows that the N-terminal part of the oxygenase domain is essential for the dimer formation of the enzyme (33). Deletion of about 100 amino acid residues of the oxygenase domain completely abolishes the dimer formation of NOS (34, 35). In addition to the dimerization of the oxygenase domain, the PDZ domain of nNOS also forms a homodimer.[5] The PDZ domain and the oxygenase domain are linked with a long stretch of unstructured PIN-binding domain. Because the PIN-binding region and the essential dimerization region of the oxygenase domain are located next to each other, it is possible that PIN binding induces structural changes to the PIN-binding region of nNOS, and such structural changes are transmitted to the oxygenase domain of the enzyme and thereby result in a dissociation/destabilization of its dimer structure (Fig. 9). The binding of PIN to nNOS is unlikely to have any effect on the dimer structure of the PDZ domain because the PDZ domain and the PIN-binding peptide fragment of nNOS are connected with a flexible linker at least 68-residues long. One should be able to prove or refute the proposed inhibition model shown in Fig. 9 by inserting a flexible linker between the PIN-binding region and the oxygenase domain of the enzyme. If the model is correct, the nNOS mutant carrying the flexible linker should no longer be susceptible to PIN inhibition. Work is in progress in our laboratory to further test this model.

[5] Q. Zhang and M. Zhang, unpublished results.

Acknowledgments—We thank Prof. Jerry Wang and Dr. James Hackett for critical comments of the manuscript.

REFERENCES

1. Rand, M. J., and Li, C. G. (1995) *Annu. Rev. Physiol.* **57,** 659–682
2. Garthwaite, J., and Boulton, C. L. (1995) *Annu. Rev. Physiol.* **57,** 683–706
3. Brenman, J. E., and Bredt, D. S. (1996) *Methods Enzymol.* **269,** 119–129
4. Bredt, D. S., and Snyder, S. H. (1994) *Neuron* **13,** 301–313
5. Williams, C. V., Nordquist, D., and McLoon, S. C. (1994) *J. Neurosci.* **14,** 1746–1755
6. Wu, H. H., Willams, C. V., and McLoon, S. C. (1994) *Science* **265,** 1593–1596
7. Lipton, S. A., and Rosenberg, P. A. (1994) *N. Engl. J. Med.* **330,** 613–622
8. Samdani, A. F., Dawson, T. M., and Dawson, V. L. (1997) *Stroke* **28,** 1283–1288
9. Iadecola, C. (1997) *Trends Neurosci.* **20,** 132–139
10. Huang, Z., Huang, P. L., Panahian, N., Dalkara, T., Fishman, M. C., and Moskowitz, M. A. (1994) *Science* **265,** 1883–1885
11. Dawson, V. L., Kizushi, V., Huang, P. L., Snyder, S. H., and Dawson, T. M. (1996) *J. Neurosci.* **16,** 2479–2487
12. Bredt, D. S., and Snyder, S. H. (1990) *Proc. Natl. Acad. Sci. U. S. A.* **87,** 682–685
13. Aoki, C., Rhee, J., Lubin, M., and Dawson, T. M. (1997) *Brain Res.* **750,** 25–40
14. Brenman, J. E., Chao, D. S., Gee, S. H., McGee, A. W., Craven, S., Santillano, D. R., Wu, Z., Huang, F., Xia, H., Peters, M. F., Froehner, S. C., and Bredt, D. S. (1996) *Cell* **84,** 757–767
15. Brenman, J. E., Christopherson, K. S., Craven, S., McGee, A. W., and Bredt, D. S. (1996) *J. Neurosci.* **16,** 7407–7415
16. Jaffrey, S. R., and Snyder, S. H. (1996) *Science* **274,** 774–777
17. Greenwood, M. T., Guo, Y., and Kumar, U. (1997) *Biochem. Biophys. Res. Commun.* **238,** 617–621
18. Gillardon, F., Krep, H., Brinker, G., Lenz, C., Böttiger, B., and Hossmann, K.-A. (1998) *Neurosci.* **84,** 81–88
19. Laue, T. L., Shah, B. D., Ridgeway, T. M., and Pelletier, S. L. (1992) in *Analytical Ultracentrifugation in Biochemistry and Polymer Science* (Harding, S. E., Rowe, A. J., and Horton, J. C., eds) pp. 90–125, The Royal Society of Chemistry, London
20. Kay, L. E., Keifer, P., and Saarinen, T. (1992) *J. Am. Chem. Soc.* **114,** 10663–10665
21. Witterkind M., and Mueller L. (1993) *J. Magn. Reson.* **B101,** 201–205
22. Grzesiek, S., and Bax, A. (1992) *J. Am. Chem. Soc.* **114,** 6291–6293
23. Zhang, O., Kay, L. E., Oliver, J. P., and Forman-Kay, J. D. (1994) *J. Biomol. NMR* **4,** 845–858
24. Delaglio, F., Grzesiek, S., Vuister, W., Zhu, G., Pfeifer, J., and Bax, A. (1995) *J. Biomol. NMR* **6,** 277–293
25. Wishart, D. S., and Sykes, B. D. (1994) *Methods Enzymol.* **239,** 363–392
26. Benashski, S. E., Harrison, A, Patel-King, R. S., and King, S. (1997) *J. Biol. Chem.* **272,** 20929–20935
27. McCaldon, P., and Argos, P. (1988) *Proteins* **4,** 99–122
28. King, S. M., and Patel-King, R. S. (1995) *J. Biol. Chem.* **270,** 11445–11452
29. King, S. M., Barbarese, E., Dillman, J. F., III, Patel-King, R. S., Carson, J. H., and Pfister, K. K. (1996) *J. Biol. Chem.* **271,** 19358–19366
30. Espreafico, E. M., Cheney, R. E., Larson, R. E., Matteoli, M., Nascimento, A. A., De Camilli, P. V., and Mooseker, M. S. (1992) *J. Cell Biol.* **119,** 1541–1557
31. Zhang, M., and Yuan, T. (1998) *Biochem. Cell Biol.*, in press
32. Stuehr, D. J. (1997) *Annu. Rev. Pharmacol. Toxicol.* **37,** 339–359
33. Crane, B. R., Arvai, A. S., Ghosh, D. K., Wu. C., Getzoff, E. D., Stuehr, D. J., and Tainer, J. A. (1998) *Science* **279,** 2121–2126
34. Crane, B. R., Arvai, A. S., Gachhui, R., Wu. C., Ghosh, D. K., Getzoff, E. D., Stuehr, D. J., and Tainer, J. A. (1997) *Science* **278,** 425–431
35. Ghosh, D. K., Wu, C., Pitters, E., Moloney, M., Werner, E. R., Mayer, B., and Stuehr, D. J. (1997) *Biochemistry* **36,** 10609–10619
36. Tochio, H., Ohki, S., Zhang, Q., Li, M., and Zhang, M. (1998) *Nat. Struct. Biol.* **5,** 965–969